https://doi.org/10.5194/essd-2023-220
Preprint. Discussion started: 12 July 2023

Open Access Earth System Science Data Discussions

A coarse pixel scale ground "truth" dataset based on the global *in situ* site measurements to support validation and bias correction of satellite surface albedo products

Fei Pan[1], Xiaodan Wu[1], Rongqi Tang[1], Qicheng Zeng[1], Zheng Li[1], Jingping Wang[1], Dongqin You[2], Jianguang Wen[2,3], and Qing Xiao[2,3]

[1]College of Earth and Environmental Sciences, Lanzhou University, Lanzhou 730000, China

[2]State Key Laboratory of Remote Sensing Science, Aerospace Information Research Institute, Chinese Academy of Sciences

[3]University of Chinese Academy of Sciences, Beijing 100049, China

Correspondence to: Xiaodan Wu (wuxd@lzu.edu.cn)

Abstract- In situ measurements from sparsely distributed networks worldwide are a valuable source of the reference data for validating or correcting the bias of satellite products. However, the significant differences in spatial scale between in situ and satellite measurements make them incomparable except for that the underlying surface of in situ sites is absolutely homogeneous. Instead, in site measurements need to be upscaled to be matched with satellite pixel. Based on the upscaling model we proposed as well as the consideration that in-situ observation generally lacks spatial representativeness due to the widely distributed spatial heterogeneity, we have developed a coarse pixel-scale ground "truth" dataset based on ground measurements of 368 in situ sites from the sparsely distributed observation networks. Furthermore, the effectiveness of the dataset was carefully evaluated over the sites with different degrees of spatial representativeness. The results demonstrate that using this dataset in validation outperforms the direct comparison between satellite and in situ site measurements. The accuracy of the reference data employed for validation or bias correction can be enhanced by 3.5% overall with this dataset. But the performance of the dataset show dependence on the degree of spatial heterogeneity. Specifically, the improvement of accuracy was the most significant over the regions with strong spatial heterogeneity, with the accuracy of reference data enhanced by 7.3%. To the best of our knowledge, this dataset is unique in providing coarse pixel scale ground truth with the

https://doi.org/10.5194/essd-2023-220
Preprint. Discussion started: 12 July 2023

widest spatial distribution and longest time series. Its ability to capture both spatial and temporal variations of surface albedo at coarse spatial scales makes it an invaluable resource for validating and correcting global surface albedo products.

1. Introduction

Surface albedo is an important variable in climate and biogeochemical models because it determines the amount of energy absorbed by the earth surface. Coarse-pixel (i.e., with a km pixel scale) satellite albedo products such as MODIS and NPP VIIRS have been widely used to tackle with global challenges and support a range of initiatives (e.g., The Paris Agreement and Sustainable Development Goals). However, satellite albedo products generally suffer from different degrees of errors due to the error of satellite observation data and the limitation of inversion algorithm, and the error of remote sensing product brings great uncertainty to the next application of the product. Taking albedo as an example, the change of albedo of 11% will cause a fluctuation of surface net radiation of 3.5 Wm-2 on global and annual averages (GCOS, 2011), which in turn will cause the change in global temperature of 0.1K. An increase of 0.00106± 0.00008 (mean ±standard deviation) of albedo will cause the radiation at the top of the atmosphere to cool by -0.15±0.1 Wm-2 (Ghimire et al., 2014). Therefore, it is very important to evaluate the uncertainty of remote sensing albedo products. In particular, when the error is relatively large, it is urgent to correct the error of remote sensing albedo products to improve the application accuracy of remote sensing products.

Both the validation and correction of remote sensing products depend on the reference data which can represent the ground truth on the coarse pixel scale. Ground measurement is usually regarded as the truth of the target variable on the observation scale. However, due to the scale mismatch between ground measurement and satellite pixel as well as the widely distributed spatial heterogeneity, ground measurement can not be directly used as the absolute truth on the pixel scale (Wu et al., 2019). Limited by the means and methods of ground measurement, the absolute truth on the coarse pixel scale can not be obtained. Instead, its best approximation value can be obtained. What we can do is to get the pixel scale relative truth close to the absolute truth as accurately as possible (Wu et al., 2019). For conciseness, the pixel scale relative truth is described as pixel scale truth in this paper.

The sparsely distributed in situ sites (i.e., at most one site within a specific product grid cell) from the networks such as FLUXNET, BSRN, and SURFRAD provide an important data source for the validation of remote sensing albedo products.(Chu et al.,

https://doi.org/10.5194/essd-2023-220
Preprint. Discussion started: 12 July 2023

2021; Augustine et al., 2000; Driemel et al., 2018). However, in situ measurements cannot be directly used as the coarse pixel scale truth given that the footprint of in situ sites is far less than the scale of a coarse pixel. A practical method of using in situ site measurements as the coarse pixel scale truth is to conduct the spatial representativeness assessment of in situ sites (Román et al., 2009; Wang et al., 2014; Moustafa et al., 2017). However, since these in situ sites were not originally established for the validation or bias correction of satellite products, only a small part of them was proved to be spatially representative, and most of them were rejected. Even for the representative site, the representativeness errors of in situ measurements are still inevitable, because land surface are not absolutely homogeneous throughout the year (Colliander et al., 2017; Xu et al., 2018; Lei et al., 2018; Williamson et al., 2018). Consequently, the representative in situ measurements are only limited to a few locations on the globe and cover discrete time periods, which cannot support a comprehensive validation and bias correction over a wide range of conditions (Loew et al., 2016).

To overcome the representative errors of in situ measurements and promote utilization ratio of in situ sites from these sparse networks in validation, Wu et al. (2020) have proposed an upscaling method specified for the single site in situ measurements. However, the effectiveness of this method has not been comprehensively assessed and its transferability to in situ sites all over the world is still unknown. In this study, we first evaluated the performance of the upscaling model over the 368 in situ sites throughout the world. Then the pixel scale ground truth data with a spatial resolution of 0.5 km were produced based on these in situ measurements. Finally, the potential usage of this dataset was discussed. As far as we know, this dataset is unique in providing coarse pixel scale ground truth with the widest spatial distribution and longest time series.

2. The experimental data

2.1 In situ site observation

In this study, in situ sites from Surface Radiation (SURFRAD), Baseline Surface Radiation Network (BSRN), AmeriFlux, EuropFlux, HiwaterWSN (Che et al., 2019), and Huailai station (Li et al., 2016; Ma et al., 2013), were utilized to generate the coarse pixel scale "truth" dataset. The spatial distribution of these in situ sites is displayed in Fig. 1. It can be seen that these sites are unevenly distributed, with most of them concentrated in the Northern Hemisphere. With consideration of the completeness and

https://doi.org/10.5194/essd-2023-220
Preprint. Discussion started: 12 July 2023

the quality of in situ observations, a total of 368 sites were selected in this study, which covers the main vegetation functional types and climatic regions (Fig. 2). The wide spread of in situ sites enables a good representation of Earth's surface.

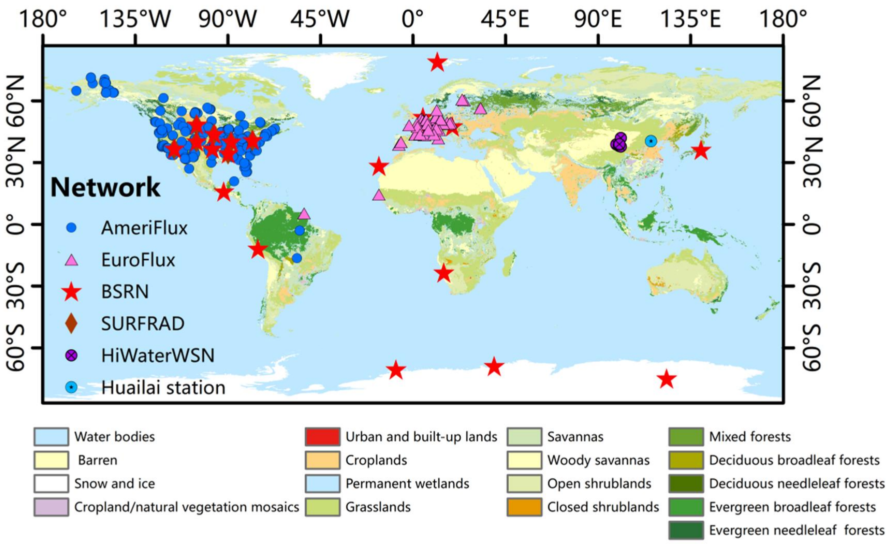

Figure 1. Global distribution of the 368 sites over different land cover types.

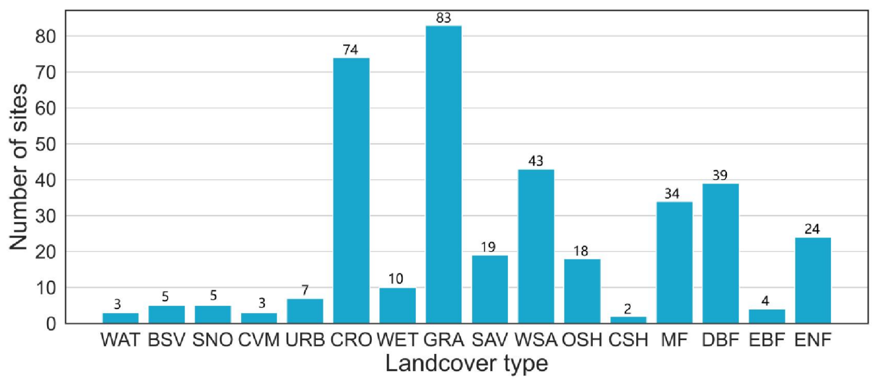

Figure 2. The distribution of stations across fifteen Land cover types indicated by International Geosphere-Biosphere Programme (IGBP). WAT, BSV, SNO, CVM, URB, CRO, WET, GRA, SAV, WSA, OSH, CSH, MF, DBF, EBF, and ENF are the abbreviation of water bodies, Barren, snow and ice, cropland/natural vegetation mosaics, urban and built-up lands, cropland permanent wetlands, grassland, savanna, woody savanna, open shrubland, closed shrublands, mixed forest, deciduous broadleaf forest, evergreen broadleaf forest, and evergreen needleleaf forests. The numeric value displayed above each bar in the chart indicates the total number of stations associated with the corresponding land cover type.

https://doi.org/10.5194/essd-2023-220
Preprint. Discussion started: 12 July 2023

These in situ sites were equipped with two pyranometers mounted back-to-back, one pointed downward and the other upward, measuring the downward radiation and upward radiation (Song et al., 2019). It is important to note that the footprint of in situ sites is not fixed, given that the measurement height of the albedometers from the underlying surface varies from site to site (Marion, 2021; Song et al., 2019). These radiometers have been rigorously calibrated and continuously supervised to reduce systematic measurement errors(Jia et al., 2013; Wang et al., 2009; Zhou et al., 2016). In situ site measured albedo of the local solar noon was calculated using the ratio of the mean upward radiation to the mean downward radiation between 11:00 a.m. and 1:00 p.m. local time as suggested by Lin et al. (2022).

2.2 The high-resolution albedo

The high-resolution albedo data were used in this study for two purposes. One is to calculate the upscaling coefficients for in situ measurements since they can capture the spatial variation characteristics of surface albedo within the coarse pixel extent. The other is to serve as the reference data because they can represent the coarse pixel albedo after aggregation. Landsat7 ETM+ images were used to generate high-resolution albedo due to their high spatial resolution of 30 m. This satellite has a revisit period of 16 days and an inclination of 98.2°, making it possible to acquire data up to a latitude of 82° N (Rösel et al., 2011).

The Landsat Level-2 reflectance data, which have been atmospherically and geometrically corrected (Teixeira et al., 2020), were used in this study. Furthermore, additional processing such as cloud screening (with Fmask algorithm) and cloud removal (with Cloud-removal-by-Synthesis (CRS) algorithm) was also carried out to further enhance the quality of the surface reflectance data. The retrieval of high-resolution surface albedo was based on the algorithm proposed by Liang et al. (2001), which provided narrowband-to-broadband conversion coefficients (Eq. (1)) for albedo retrieval from Landsat7 ETM+ using spectral reflectance library and simulations under different atmospheric and surface conditions under the Lambertian assumption. The anticipated accuracy of this algorithm approximates 0.02 (Liang, 2001). This equation provides a valuable tool for the accurate estimation of surface albedo from satellite data and has been widely used in numerous studies on land surface processes and global climate change.

$$\alpha_{short} = 0.356\alpha_1 + 0.130\alpha_3 + 0.373\alpha_4 + 0.085\alpha_5 + 0.072\alpha_7 - 0.0018 \quad (1)$$

where α_{short} denotes the shortwave surface albedo, and α_i denotes the spectral

https://doi.org/10.5194/essd-2023-220
Preprint. Discussion started: 12 July 2023

albedo at the wavelength of ith satellite spectral band.

2.3 Coarse pixel-scale satellite albedo product

The MCD43A3 V061 product was used in this paper to serve as an example of coarse pixel satellite albedo products due to its wide acceptance. The shortwave (3000-5000 nm) albedo was extracted to match the spectral range of in situ-measured albedo. It provides black sky albedo (BSA) and white sky albedo (WSA) with a spatial resolution of 500 m and a temporal resolution of daily (Schaaf et al., 2002). The BSA and WSA can be linearly combined with the sky diffuse light ratio to derive the blue-sky albedo in the actual environment (Pinty et al., 2005).

$$\alpha = \alpha_{WSA} \times r + \alpha_{BSA} \times (1 - r) \tag{2}$$

where α, α_{WSA}, and α_{BSA} represent the blue-sky albedo, WSA, and BSA of MCD43A3, respectively. The actual sky diffuse light ratio r can be calculated using equation (3) as suggested by Stokes and Schwartz (1994).

$$r = 0.122 + 0.85 \times \exp(-4.8 \times \cos\theta) \tag{3}$$

where θ denotes the solar zenith angle at local solar noon.

2.4 The ancillary dataset

The auxiliary data were used in this paper to explore the potential influence factors on the accuracy of the pixel scale ground truth data. Several common surface parameters, including elevation, land cover types, and spatial heterogeneity, were considered. DEM data were obtained from the Multi-Error-Removed Improved-Terrain (MERIT) Digital Elevation Model (DEM) (Mcclean et al., 2020; Yamazaki et al., 2017), with a high horizontal resolution of three arc-seconds (approximately 90 meters). The MERIT DEM was produced using the advanced algorithms of HydroSHEDS (Hydrological data and maps based on SHuttle Elevation Derivatives at multiple Scales) to remove various types of errors in existing DEMs, such as voids, noise, and artifacts (Uuemaa et al., 2020). The MCD12Q1 product provides global land cover type information with a spatial resolution of 500 m at an annual time step from 2012 to 2018. It provides information on 17 different land cover types, making it a valuable data source for many applications. It is important to point out that there is a slight difference regarding the land cover information between the data of different years. Here, we have used the land cover type with the highest degree of agreement between the data in different years.

https://doi.org/10.5194/essd-2023-220
Preprint. Discussion started: 12 July 2023

Open Access Earth System Science Data Discussions

Spatial heterogeneity is a critical factor influencing the spatial scale match between in situ and satellite measurements because it reduces the spatial representativeness of in situ measurements (Wu et al., 2022). It refers to the uneven distribution of surface albedo within the coarse pixel. A pixel that exhibits spatial heterogeneity denotes that the value of surface albedo at one location is different from that of other locations. To quantify the spatial heterogeneity of surface albedo within a coarse pixel, the spatial variability (standard deviation, Std) of all subpixel albedos within a coarse pixel was calculated (Colliander et al., 2017; Jin et al., 2003). Here, the subpixel albedos denote the high-resolution pixel albedo within the coarse pixel.

$$Std = \sqrt{\frac{1}{L-1}\sum_{i=1}^{L}(Z_i - \overline{Z})^2} \quad (4)$$

where Z_i denotes the high-resolution albedo and $\overline{Z}$ is the averaged albedo of all high-resolution albedos within the extent of the coarse pixel. L refers to the number of high-resolution albedo pixels with a coarse pixel.

3. Methodology

3.1 The upscaling model specified for single in situ site measurements

In situ measurements taken at a single in situ site can provide accurate measurements on the point scale and offer continuous temporal variation information for long time series. But they are insufficient to represent albedo at the coarse-pixel scale due to the spatial heterogeneity within the coarse pixel. High-resolution albedo maps can capture the spatial variation information within the coarse pixel. The basic idea of the upscaling model is to derive the upscaling coefficients based on high-resolution albedo maps and then applied these upscaling coefficients to long-term in situ measurements (Wu et al., 2020). In this way, both the spatial variation information and the temporal variation information of surface albedo can be captured through the combination of high-resolution albedo maps and long time series in situ measurements, deriving the long time series pixel scale ground truth data.

Since the high-resolution albedo maps serve as an important linkage between in situ measurement scale and satellite coarse pixel scale, they should meet several acquirements. First, its spatial resolution should be equal or close to the footprint of in situ measurements, because the upscaling coefficients were determined by long time series high-resolution albedo maps and then were applied to in situ measurements. Second, the high-resolution albedo maps should cover at least one full cycle period, which is typically one year, to account for the seasonal variations of surface heterogeneity caused by phenology, because the upscaling coefficients will be applied to long time series in situ measurements. In this study, the Landsat7 ETM+ albedo maps from 2012 to 2018 were processed to capture the spatiotemporal variation of surface albedo and used as prior knowledge for deriving the upscaling coefficients.

The upscaling coeffcients were calculated for each subpixel within the coarse pixel extent by establishing a regression relationship between one subpixel albedo time series and the subpixel albedo time series corresponding to the in situ site (Eq. (4)). To avoid the uncertainty caused by different data sources, both of them were simulated by Landsat7 albedo. Using the same data source can reduce the influence of errors of Landsat7 ETM+ albedo to a certain extent.

$$\theta_{ETM+}(\mathrm{x,y,d}) = \mathrm{W(x,y)^T}\theta_{ETM+\_in\ situ}(\mathrm{d}) \tag{4}$$

and

$$\theta_{ETM+\_in\ situ'}(d) = [1, \theta_{ETM+\_in\ situ}(d)]^T \tag{5}$$

where x and y correspond to the location of a single Landsat7 ETM+ pixel within a coarse pixel, while d denotes the date of the Landsat7 ETM+ albedo map. $\theta_{\mathrm{ETM+}}$ denotes the individual Landsat7 ETM+ pixel within a coarse pixel. $\theta_{\mathrm{ETM+\_in\ situ}}$ indicates the Landsat7 ETM+ pixel albedo time series corresponding to the in situ site. The vector W represents the upscaling coefficients to be derived.

To ensure a robust estimation, a cost function J is established by combining all the Landsat7 ETM+ albedo data throughout the whole time series (i.e., 2012-2018).

$$\mathrm{J} = \min\{\textstyle\sum_{\mathrm{d=1}}^{\mathrm{L}}[\theta_{ETM+}(\mathrm{x,y,d}) - \mathrm{W(x,y)^T}\theta_{ETM+\_in\ situ'}(\mathrm{d})]^2\} \tag{6}$$

Using the ordinary least-squares (OLS) algorithm, the vector of coefficients W can be obtained by minimizing the cost function.

$$\mathrm{W(x,y)} = [\theta_{ETM+\_in\ situ'}^{\mathrm{T}}\theta_{ETM+\_in\ situ'}]^{-1}\theta_{ETM+\_in\ situ'}^{\mathrm{T}}\theta_{ETM+}(\mathrm{x,y}) \tag{7}$$

After the upscaling coefficients were acquired, they were applied to in situ site measurements to simulate the in situ reporting of surface albedo over each Landsat7 ETM+ pixel ($\theta_{in\ situ\ ETM+}$) within the coarse pixel:

$$\theta_{in\ situ\ ETM+}(x,y,d) = W(x,y)^T\theta_{in\ situ}(d) \tag{8}$$

Then the coarse pixel ground truth ($\theta_{in\ situ\_ref}$) can be derived by aggregating all the $\theta_{in\ situ\ ETM+}$ within the coarse pixel using the point spread function (PSF) of the MODIS albedo characterized by Peng et al. (2015).

https://doi.org/10.5194/essd-2023-220
Preprint. Discussion started: 12 July 2023

$$\theta_{in\ situ\_ref}(d) = \frac{\int_{(x,y)\in D} f_{PSF}(x,y)\theta_{in\ situ\ ETM+}(x,y,d)}{\int_{(x,y)\in D} f_{PSF}(x,y)} \tag{9}$$

where D denotes the spatial extent of the coarse pixel, and f_{PSF} represents the PSF.

As shown in Eq. (8-9), it can be seen that the upscaling coefficients are time-independent and can be applied to in situ measurements throughout the entire time series under the condition that there are no sudden changes such as wildfires and deforestation on the land surfaces. It is noteworthy that a high-resolution albedo map is no longer a prerequisite for the practical upscaling process once the upscaling coefficients have been obtained.

3.2 The evaluation of upscaling models and pixel scale ground truth

3.2.1 The evaluation of the upscaling model

As explained above, the key to the upscaling method is to obtain upscaling coefficients based on 30-meter Landsat7 ETM+ albedo data from 2012 to 2018. Hence, the accuracy of the upscaling model is highly dependent on the performance of the upscaling coefficients. Inspired by the evaluation method proposed by Wu et al. (2016), the accuracy of upscaling coefficients were assessed using the Landsat7 ETM+ albedo data from 2019 to 2021. The upscaling results with the upscaling coefficients can be determined with the Eqs. (10-11). The reference value on the coarse pixel scale is the aggregated Landsat7 ETM+ albedo at the 500 m resolution as recommended by Wu et al. (2016) (Eq. (12)).

$$\theta_{RETM+}(x,y,d) = W(x,y)^T \theta_{ETM+}(d) \tag{10}$$

$$\theta_{upscaling}(d) = \frac{\int_{(x,y)\in D} f_{PSF}(x,y)\theta_{RETM+}(x,y,d)}{\int_{(x,y)\in D} f_{PSF}(x,y)} \tag{11}$$

$$\theta_{reference}(d) = \frac{\int_{(x,y)\in D} f_{PSF}(x,y)\theta_{ETM+}(x,y,d)}{\int_{(x,y)\in D} f_{PSF}(x,y)} \tag{12}$$

where θ_{RETM+} is the reporting of surface albedo over each Landsat7 ETM+ pixel based on the Landsat7 ETM+ pixel albedo corresponding to the in situ sites and the upscaling

https://doi.org/10.5194/essd-2023-220
Preprint. Discussion started: 12 July 2023

coefficients. $\theta_{upscaling}$ denote the upscaling results and $\theta_{reference}$ represent the reference value.

The similarity and consistency between the $\theta_{upscaling}$ and $\theta_{reference}$ were evaluated by three metrics: bias, coefficient of determination (R^2), and root-mean-square error (RMSE).

$$\mathrm{RMSE} = \sqrt{\sum_{\mathrm{d}=1}^{\mathrm{L}}(\theta_{upscaling}(\mathrm{d}) - \theta_{reference}(\mathrm{d}))^2/\mathrm{L}} \tag{10}$$

$$\mathrm{Bias} = \sum_{\mathrm{d}=1}^{\mathrm{L}}(\theta_{upscaling}(\mathrm{d}) - \theta_{reference}(\mathrm{d}))/\mathrm{L} \tag{11}$$

$$\mathrm{R} = \frac{\sum_{\mathrm{d}=1}^{\mathrm{L}}(\theta_{upscaling}(\mathrm{d})-\overline{\theta_{upscaling}})(\theta_{reference}(\mathrm{d})-\overline{\theta_{reference}})}{[\sum_{\mathrm{d}=1}^{\mathrm{L}}(\theta_{upscaling}(\mathrm{d})-\overline{\theta_{upscaling}})^2\sum_{\mathrm{d}=1}^{\mathrm{l}}(\theta_{reference}(\mathrm{d})-\overline{\theta_{reference}})^2]^{1/2}} \tag{12}$$

3.2.2 Assessment of pixel scale ground truth

The way of evaluating the pixel scale ground truth is similar to that of the upscaling model. Namely, the accuracy of $\theta_{in\ situ\_ref}$ was assessed through the comparison with $\theta_{reference}$. Furthermore, the performance of the pixel scale ground truth is also compared to that of single in situ site measurements. To eliminate the influence of the magnitude of surface albedo on accuracy indicators, the relative root-mean-square error (RRMSE) was used here, which is defined as the ratio of RMSE to the mean value of surface albedo on the coarse pixel scale.

$$\mathrm{RRMSE} = \frac{RMSE}{\overline{\theta_{in\ situ\_ref}}} \times 100\% \tag{13}$$

where $\overline{\theta_{in\ situ\_ref}}$ represents the mean value of coarse pixel-scale albedo truth, and L denotes the length of the temporal sequence of data.

4. Results and Discussion

4.1 The performance of the upscaling model

The performance of the upscaling coeffcieints has been comprehensively evaluated over the 368 in situ sites. The wide spread of in situ sites across different elevations, different land cover types, and different degrees of spatial heterogeneity can ensure the objectivity of the evaluation results. To show the agreement between $\theta_{upscaling}$ and $\theta_{reference}$ more intuitively, we present the scatterplots between them in Fig. 2. As shown in Fig. 3, the scatterplots between $\theta_{upscaling}$ and $\theta_{reference}$ are generally distributed around the 1:1 line, with R^2 close to 0.9. The upscaling coefficients show no

https://doi.org/10.5194/essd-2023-220
Preprint. Discussion started: 12 July 2023

Open Access Earth System Science Data Discussions

systematic error, indicated by the biases close to 0. However, the performance of the upscaling models is site dependent. For instance, the accuracy of the upscaling results over the US-Ha2 site obviously outperforms that of the IT-Tor site (Fig. 2(c vs. f)). To fully understand the performance of upscaling coefficients in different conditions, the accuracy indicators of the upscaling coefficients throughout these 368 in situ sites were summarized as the histograms (Fig. 3).

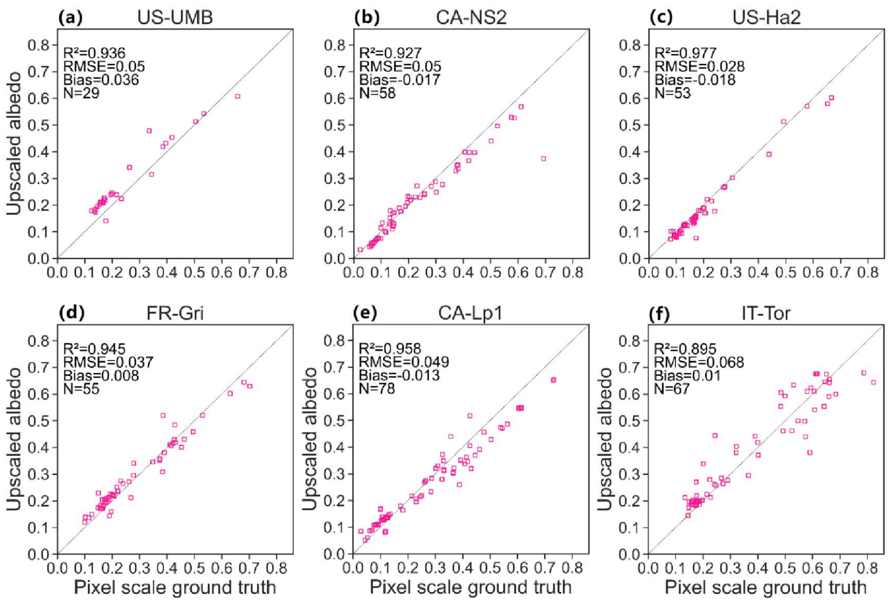

Figure 3. The scatter plots between the upscaling results with the upscaling models and the coarse pixel scale reference. Only parts of the results are shown for conciseness. Specifically, only one in situ site is shown for each land cover type.

Based on the results presented in Fig. 4, it can be seen that the overall accuracy of the upscaling coefficients is satisfactory. The biases are concentrated in 0, and more than 90% of them are within the range of ±0.02 (Fig. 4(b)). The highest density of R^2 is between 0.9 and 1 as shown in Fig. 4(c), and only a small part of the sites show a relatively small R^2 of lower than 0.8 but larger than 0.5. Nevertheless, it should be noted that those sites exhibit a more scattered distribution of RMSE values, with a maximum of 0.1 and a minimum of 0.01 (Fig. 4(a)). The highest density is between 0.03 and 0.05 for RMSE.

https://doi.org/10.5194/essd-2023-220
Preprint. Discussion started: 12 July 2023

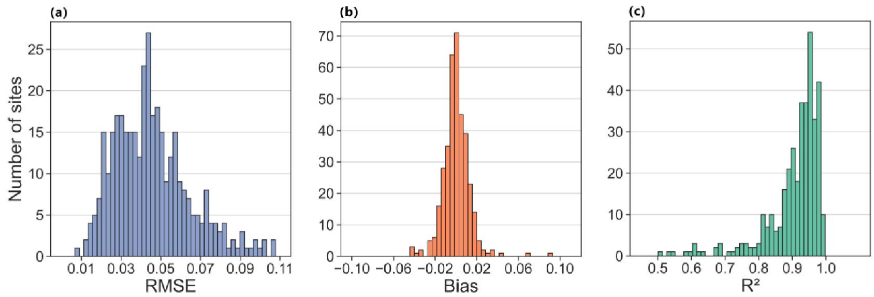

Figure 4. Distribution of RMSE (a), Bias (b), and R^2 (c) of the upscaling coefficients. The histograms presented here combine the results of the 368 in situ sites.

Given the fact that the accuracy of the upscaling models shows great variability, it is necessary to explore the influence factors on the performance of the upscaling models. In this study, the effect of land cover type, elevation, and spatial heterogeneity were considered. The influence of spatial heterogeneity on the accuracy of the upscaling model is displayed in Fig. 5. The RMSE exhibits a significant positive correlation with spatial heterogeneity (Fig. 5(a)), with superior performance often observed in areas with lower spatial heterogeneity. Similarly, the R^2 of different sites typically decreases with the increase of spatial heterogeneity (Fig. 5(b)). It is worth noting that when the spatial heterogeneity exceeds 0.1, the model's stability fluctuates considerably, indicated by the larger height of the boxplots of RMSE and R^2. Based on these results, it can be seen that spatial heterogeneity has enormous implications for the performance of the upscaling models. One possible reason is that the assumption of a linear relationship between the subpixel albedo of other locations and the subpixel albedo containing the in situ site cannot be satisfied over the surface with large spatial heterogeneity.

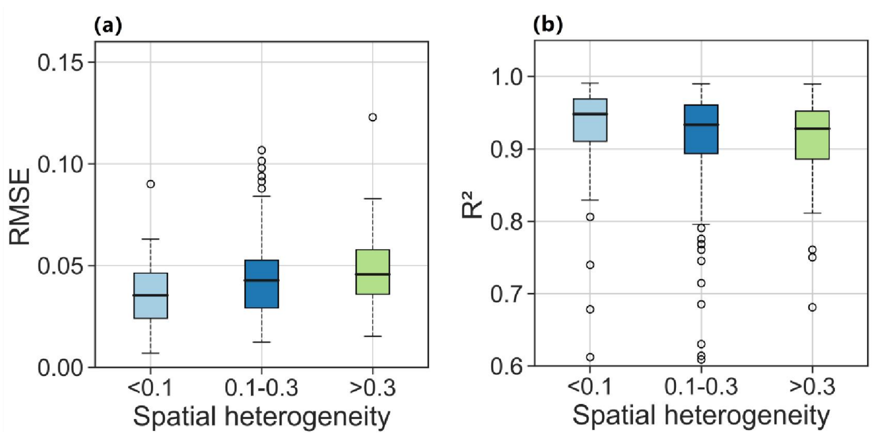

Figure 5. Boxplots showing the dependence of RMSE (a) and R^2 (b) of the upscaled albedo on spatial heterogeneity. Three different degrees of spatial heterogeneity are marked by different colors.

https://doi.org/10.5194/essd-2023-220
Preprint. Discussion started: 12 July 2023

The variation of RMSE and R^2 of upscaling models with elevation is shown in Fig. 6. It is interesting to see that the upscaling model presents the highest accuracy for elevations below sea level, with the lowest RMSE around 0.3 and the highest R^2 exceeding 0.95. By contrast, the model's performance was the worst for elevations above 2500 meters, displaying the highest RMSE and the lowest R^2. However, for the areas with elevation between 0 m and 2500 m, the variation trend of RMSE and R^2 with elevation is not obvious. For instance, a slightly decreasing trend can be found as elevation increase from 0-200 m to 500-1500 m. But a slight increasing trend appears as elevation increase from 500-1500 m to the area above 2500 m. Except for the areas below 0 m, both the RMSE and R^2 show a wide fluctuation range, indicated by the large height of their boxplots. These results demonstrate that the accuracy of the upscaling model is controlled by many other factors. The good performance of the upscaling model over the area below sea level may be attributed to the small spatial heterogeneity as shown in Fig. 7. It can be found that the area below sea level is featured by small spatial heterogeneity less than 0.1.

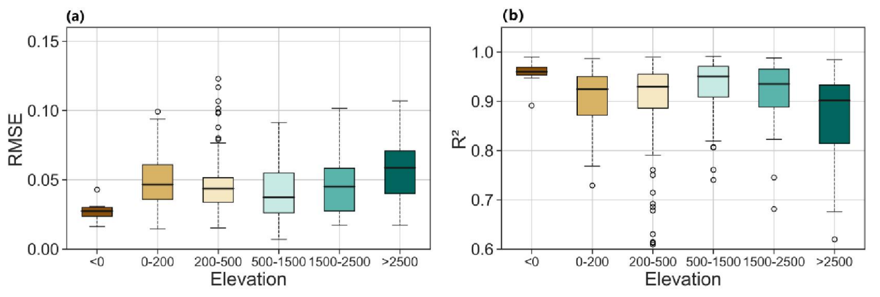

Figure 6. The variations of RMSE (a) and R^2 (b) of with elevation.

As illustrated in Fig. 7, it is evident that the RMSE exhibits a noticeable upward trend with increasing spatial heterogeneity at each elevation level. This suggests that spatial heterogeneity plays a dominant role in determining the performance of the upscaling models.. Nevertheless, the influence of spatial heterogeneity seems to be related to the elevation. From Fig. 7(a), it can be seen that the difference in RMSE between different spatial heterogeneity levels tends to be larger with the increase of elevation. A similar phenomenon can be found in R^2. For each specific level of spatial heterogeneity, the variation trend of RMSE and R^2 with elevation is not the same. For areas with small spatial heterogeneity (<0.1), their variation trend is not significant. By contrast, For the area with strong spatial heterogeneity (>0.3), the increasing/decreasing trend of RMSE/R^2 with elevation is obvious, especially for the area above 200 m.

https://doi.org/10.5194/essd-2023-220
Preprint. Discussion started: 12 July 2023

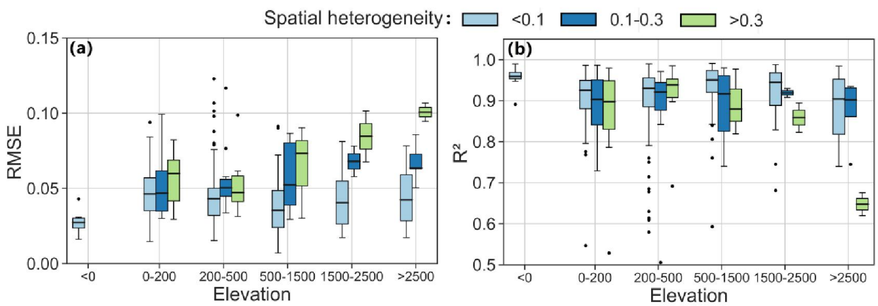

Figure 7. The plots show combined results of the RMSE (a) and R^2 (b) variations based on elevation and spatial heterogeneity.

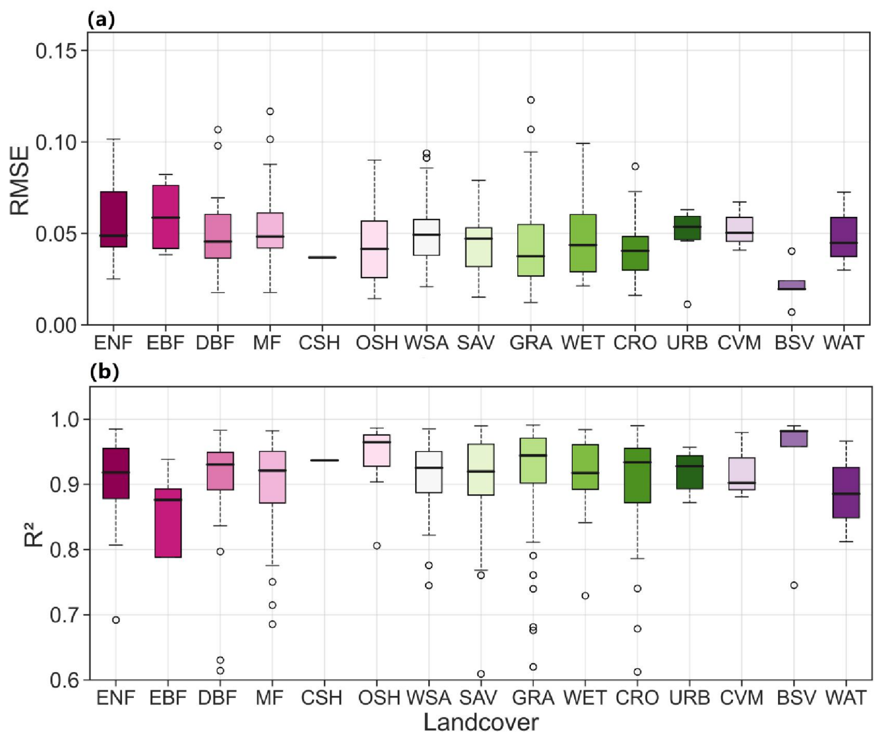

Figure 8. The variations in RMSE (a) and R^2 (b) are dependent on landcover, different colors refer to the fifteen different land cover types.

The influence of land cover types on the accuracy of the upscaling model is displayed in Fig. 8. It shows that the model's accuracy is relatively poor on EBF, with most of the RMSEs exceeding 0.05 and R^2 below 0.90. By contrast, the model performs best on bare land (BSV), with the lowest RMSE close to 0.02 and a relatively higher

R^2 around 0.97. The accuracy of the model over the remaining surface cover types was similar, with RMSE and R^2 values around 0.05 and 0.90, respectively. The boxplots of RMSE at URB, CVM, and BSV present a narrow range of values, indicating a relatively stable model performance. Conversely, the boxplots of the RMSE at ENF and EBF show a large range of values, indicating significant variability in model performance in these areas. In fact, the influence of land cover types is also associated with the effect of spatial heterogeneity. As shown in Fig. 9, the BSV is featured by small spatial heterogeneity. By contrast, a considerable number of sites over EBF show a strong spatial heterogeneity.

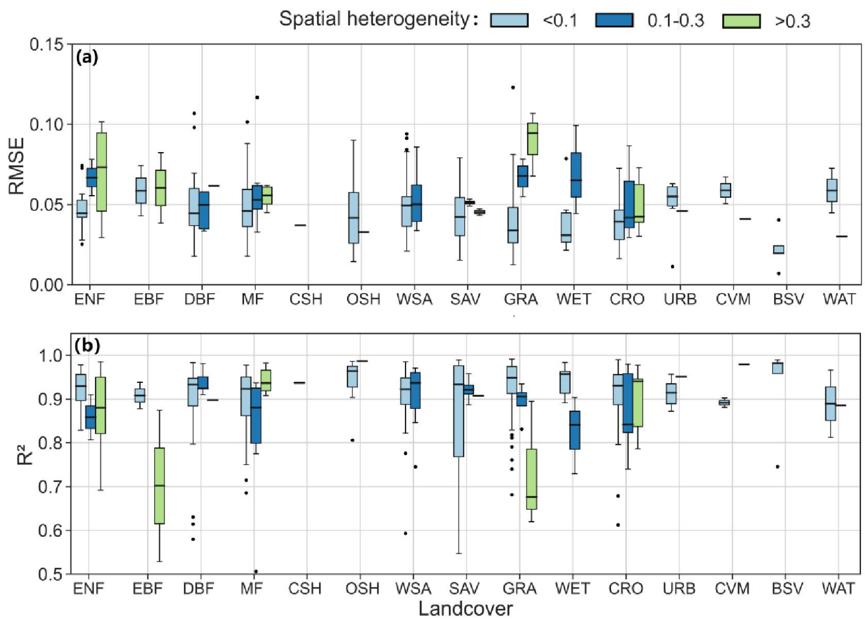

Figure 9. The plots show combined results of the RMSE (a) and R^2 (b) variations based on land cover and spatial heterogeneity.

As shown in Fig. 9(a), the RMSE of the upscaling model basically presents an increasing trend with spatial heterogeneity over each land cover type, further indicating the dominant role of spatial heterogeneity in determining the accuracy of the upscaling model. The outliers at OSH, URB, CVM, and WAT are attributed to the small number of sites with relatively larger spatial heterogeneity. Nevertheless, the influence of spatial heterogeneity show dependence on land cover type, which is most significant on GRA.

4.2 The accuracy of the pixel scale ground truth

Since there are a considerable number of in situ sites, the accuracy of pixel scale

https://doi.org/10.5194/essd-2023-220
Preprint. Discussion started: 12 July 2023

ground truth was summarized as the boxplots (Fig. 10). For comparison purposes, the errors of single site measurements when they were directly used as the pixel scale reference were also calculated and summarized as the boxplots. It can be seen that the errors of pixel scale ground truth show a slight variation with spatial heterogeneity, with the median RRMSE ranging from 29.44 % to 31.51% and then to 29.35 %, resulting in the overall RRMSE of 29.89 %. It is important to note that this variation pattern is not the same as the accuracy of the upscaling model, which shows a monotonous decrease trend with the increase of spatial heterogeneity. The wide range of the boxplots shows that the accuracy of the pixel scale ground truth is also influenced by other factors.

Indeed, the errors of the pixel scale ground truth are not negligibly small. Nevertheless, its accuracy is consistently better than the single site measurements over the surfaces with different levels of spatial heterogeneity as shown in Fig. 10. The smaller RRMSE of pixel scale ground truth (29.89 % vs. 33.34 %) indicates that this dataset can improve the accuracy of pixel scale reference data a lot compared to the single site measurements. Nevertheless, the degree of the improvement depends on the situation, which is the most significant over the sites with the strongest spatial heterogeneity, with the RRMSE decreasing from 36.62 % to 29.35 %. The in situ sites with medium spatial heterogeneity follow, with the RRMSE decreasing from 35.12 % to 31.51 %. The improvements are the smallest over the sites with the smallest spatial heterogeneity, with the RRMSE decreasing from 32.69 % to 29.44 %. Hence, it can be concluded that the degree of improvements of this dataset shows an increasing trend with spatial heterogeneity. Furthermore, the accuracy of the pixel scale ground "truth" dataset is more stable than that of the single site measurements, indicated by the smaller height of the boxplots of the former.

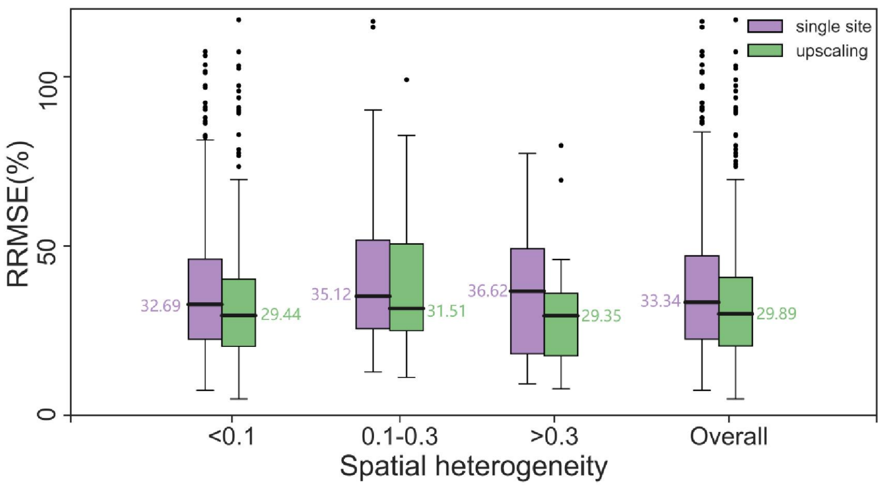

Figure 10. The boxplots of RRMSE of pixel scale ground truth and single site measurements. The boxplots are categorized by different degrees of spatial heterogeneity and overall accuracy. The median of the boxplots is indicated by the numbers around the plots.

The aforementioned results confirm the efficacy of our pixel scale ground "truth" dataset in different scenarios, which is superior to single site measurements, whether for the sites with higher or lower spatial heterogeneity. The improvement of this dataset is more significant over the heterogeneous sites. Hence, it is highly helpful over heterogeneous surfaces in the validation or bias correction of satellite albedo products.

4.3 The usage of the pixel scale ground "truth" dataset

Validation is important for both the satellite product producers and end users as it provides a quantitative evaluation of the advantage and disadvantages of satellite products. However, in situ measurements, locations, coverage, scaling, and representation, are rather diverse, resulting in a different impression of accuracy. Consequently, most of the validation results are not directly comparable, which further limits the potential utility of satellite products. As pointed out by GCOS, one possibility for addressing this challenge is through a unified and systematic validation based on a unified, standard, and consistent reference dataset. The pixel scale ground truth was obtained through a standardized operational procedure based on a large number of in situ sites' measurements distributed across the globe. Such standardization enables the fair comparison between the accuracy of different satellite products of the same ECV, thus providing a foundation for the coordinated utilization of diverse satellite albedo products and maximizing their potential capabilities. Fig. 11 presents an example for

https://doi.org/10.5194/essd-2023-220
Preprint. Discussion started: 12 July 2023

the validation of MCD43A3 V0061 based on this pixel scale ground dataset.

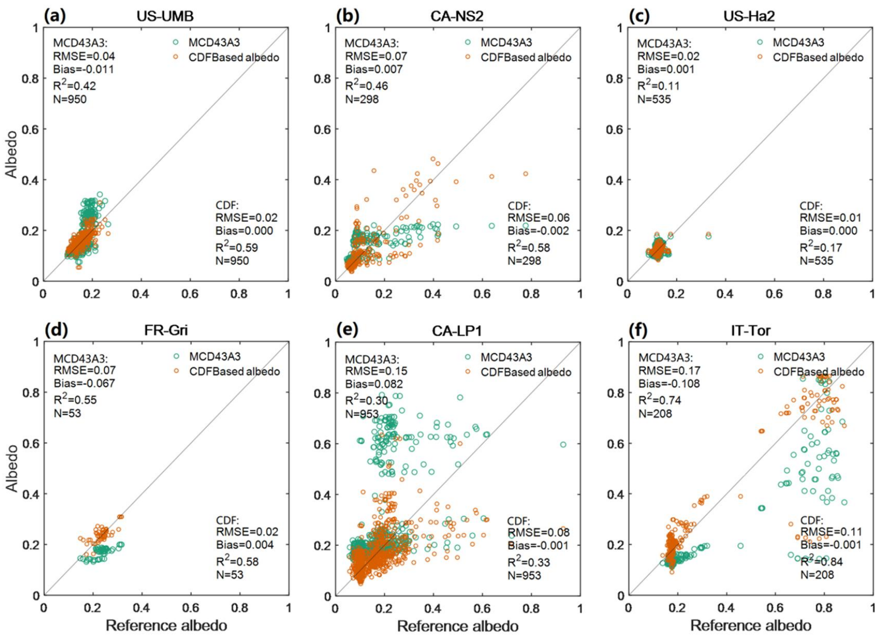

Figure 11. The scatter plots between the MCD43A3 and pixel scale ground truth (green dots) as well as the scatterplots between CDF-corrected MCD43A3 and pixel scale ground truth (brown dots).

Apart from validation, the pixel scale ground "truth" dataset can also be used as a reference to correct the bias of satellite albedo products. There have been many kinds of bias correction models (Wang et al., 2022). In this study, the CDF (cumulative distribution function) method (Calheiros et al., 1987) was utilized to correct the bias in MCD43A3 V0061 for example purposes. As shown in Fig. 10, the bias correction generally improves the accuracy of satellite albedo products, and the improvement is particularly significant for regions with strong heterogeneity (Fig. 10(d-f)). Hence, it is reasonable to consider that this dataset has the potential to further improve the quality of satellite albedo products, particularly in regions with strong surface heterogeneity.

5. Data availability

The processed coarse pixel scale ground "truth" dataset is openly accessible and can be obtained from Zenodo (https://doi.org/10.5281/zenodo.8008455; Pan et al., 2023). The dataset files are available in the machine-readable data format (.tab) and have been conveniently organized into separate folders for Ameriflux, Euroflux, BSRN, SURFRAD, HiwaterWSN, and Huailai station, facilitating easy accessibility and

https://doi.org/10.5194/essd-2023-220
Preprint. Discussion started: 12 July 2023

utilization.

6. Conclusion

Both validation and correction of remote-sensing albedo products are essential to promote the rational utilization of satellite albedo products in various scientific applications. Typically, in situ single site-based albedo measurements with a widespread are the backbone of validation and correction. However, since satellite-based albedo and tower-based albedo are generated at different spatial scales, direct comparison is only valid over specific homogeneous land surfaces. Nevertheless, spatial heterogeneity is a basic feature of most land surfaces, resulting in the limited spatial representativeness of single site measurements. Thus, the most critical aspect of validation/ correction is obtaining the pixel scale ground truth albedo based on in situ site measurements.

However, the ways of obtaining pixel scale ground truth are rather diverse regarding the in situ measurements, locations, coverage, scaling, and representation, resulting in different accuracy of pixel scale "truth" dataset. Consequently, most of the validation/correction results are not directly comparable, which further limits the further use of satellite products. A suite of continuous, independent, and representative pixel scale ground "truth" dataset of surface albedo is needed. To the best of our knowledge, there is still a lack of such a kind of dataset with global coverage. To fill this gap, we have developed a coarse pixel-scale ground truth albedo dataset based on ground measurements of 368 in situ sites from the sparsely distributed observation networks (e.g., SURFRAD, BSRN, and Fluxnet) and an upscaling model specified for the single site measurements.

The applicability of the upscaling model to the in situ site measurements was first comprehensively on a global scale. The overall accuracy of the upscaling coefficients is satisfactory, with the biases concentrated around 0. 90 % of these biases are within the range of ±0.02. The influence factors on the performance of the upscaling models were also explored. Spatial heterogeneity plays a dominant role in determining the performance of the upscaling models. But the influence of spatial heterogeneity is related to the elevation and land cover type, which tends to be larger with the increase of elevation and over the land cover type of GRA.

The accuracy of the pixel scale ground "truth" dataset was also comprehensively evaluated. The errors of pixel scale ground truth show a slight variation with spatial heterogeneity, with the median RRMSE ranging from 29.44 % to 31.51 % and then to

https://doi.org/10.5194/essd-2023-220
Preprint. Discussion started: 12 July 2023

29.35 % over the surfaces with small, medium, and large spatial heterogeneity, respectively, resulting in the overall RRMSE of 29.89 %. Although the errors of the pixel scale ground truth are not negligibly small, its accuracy is consistently better than the single site measurements over the surfaces with different levels of spatial heterogeneity. The smaller RRMSE of pixel scale ground truth compared to the single site measurements (29.89 % vs. 33.34 %) indicate that this dataset can improve the accuracy of pixel scale reference data a lot. The degree of improvements of this dataset shows an increasing trend with the spatial heterogeneity. Furthermore, the accuracy of the pixel scale ground "truth" dataset is more stable than that of the single site measurements.

The pixel scale ground truth was obtained through a standardized operational procedure. Such standardization enables the fair comparison between the accuracy of different satellite products of the same ECV. This newly introduced dataset serves as a remedy to the inadequacy and inconsistency of reference data currently employed in validation/correction efforts, thereby paving the way for the coordinated use of various satellite albedo products and unlocking the full capacity of different albedo products.

Author contributions

FP, XW was responsible for the main research ideas and writing the manuscript. JW, DY, QX contributed to the data collection. XW, RT, QZ, ZL, JW have supported the work with formal analysis, XW contributed to the manuscript organization. All authors have worked on the writing, particularly for review and editing.

Competing interests

The contact author has declared that none of the authors has any competing interests.

Disclaimer

Publisher's note: Copernicus Publications remains neutral with regard to jurisdictional claims in published maps and institutional affiliations.

Acknowledgements

The authors would like to thank the various site networks and services, namely AmeriFlux, EuroFlux, BSRN, SURFRAD, HiwaterWSN and Huailai station, for their dedicated efforts in providing the ground measurements that have contributed to the generation of the coarse pixel scale " truth" dataset.

Financial support

This work was jointly supported by the National Natural Science Foundation of China (Grant No. 41971316 and 42071296) and the Fundamental Research Funds for the Central Universities (lzujbky-2020-72).

References

Augustine, J. A., Deluisi, J. J., and Long, C. N.: SURFRAD-A National Surface Radiation Budget Network for Atmospheric Research. Bulletin of the American Meteorological Society, 81, 2341-2358. doi:10.1175/1520-0477(2000)081<2341:Sansrb>2.3.Co;2, 2000.

Calheiros, R. V., and Zawadzki, I.: Reflectivity–Rain Rate Relationships for Radar Hydrology in Brazil. Journal of Climate and Applied Meteorology, 26(1), 118-132, 1987.

Che, T., Li, X., Liu, S., Li, H., Xu, Z., Tan, J., Zhang, Y., Ren, Z., Xiao, L., Deng, J., Jin, R., Ma, M., Wang, J., and Yang, X.: Integrated hydrometeorological, snow and frozen-ground observations in the alpine region of the Heihe River Basin, China. Earth Syst. Sci. Data, 11(3), 1483-1499. doi:10.5194/essd-11-1483-2019, 2019.

Chu, H., Luo, X., Ouyang, Z., Chan, W. S., Dengel, S., Biraud, S. C., Torn, M. S., Metzger, S., Kumar, J., Arain, M. A., Arkebauer, T. J., Baldocchi, D., Bernacchi, C., Billesbach, D., Black, T. A., Blanken, P. D., Bohrer, G., Bracho, R., Brown, S., Brunsell, N. A., Chen, J., Chen, X., Clark, K., Desai, A.R., Duman, T., Durden, D., Fares, S., Forbrich, I., Gamon, J. A., Gough, C.M., Griffis, T., Helbig, M., Hollinger, D., Humphreys, E., Ikawa, H., Iwata,H., Ju, Y., Knowles, J.F., Knox, S.H., Kobayashi, H., Kolb, T., Law, B., Lee, X., Litvak, M., Liu, H., Munger, J. W., Noormets, A., Novick, K., Oberbauer, S. F., Oechel, W., Oikawa, P., Papuga, S. A., Pendall, E., Prajapati, P., Prueger, J., Quinton, W. L., Richardson, A. D., Russell, E. S., Scott, R. L., Starr, G., Staebler, R., Stoy, P. C., Stuart-Haëntjens, E., Sonnentag, O., ullivan, R. C., Suyker, A., Ueyama, M., Vargas, R., Wood, J. D., and Zona, D.: Representativeness of Eddy-Covariance flux footprints for areas surrounding AmeriFlux sites. Agricultural and Forest Meteorology, 301-302, 108350. doi:https://doi.org/10.1016/j.agrformet.2021.108350, 2021.

Colliander, A., Jackson, T. J., Bindlish, R., Chan, S., Das, N., Kim, S. B., Cosh, M.H., Dunbar, R.S., Dang, L., Pashaian, L., Asanuma, J., Aida, K., Berg, A. Rowlandson, T. Bosch, D. Caldwell, T. Caylor, K. Goodrich, D., al Jassar, H., Lopez-Baeza, E., Martínez-Fernández, J., González-Zamora, A., Livingston, S., McNairn, H., Pacheco, A., Moghaddam, M., Montzka, C., Notarnicola, C., Niedrist, G., Pellarin, T., Prueger, J., Pulliainen, J., Rautiainen, K., Ramos, J., Seyfried, M., Starks, P., Su, Z., Zeng, Y., van der Velde, R., Thibeault, M., Dorigo, W., Vreugdenhil, M., Walker, J.P., Wu, X., Monerris, A., O'Neill, P. E., Entekhabi, D., Njoku, E.G., and Yueh, S.: Validation of SMAP surface soil moisture products with core validation sites. Remote Sensing of Environment, 191, 215-231. doi:https://doi.org/10.1016/j.rse.2017.01.021, 2017.

https://doi.org/10.5194/essd-2023-220
Preprint. Discussion started: 12 July 2023

Driemel, A., Augustine, J., Behrens, K., Colle, S., Cox, C., Cuevas-Agulló, E., Denn, F. M., Duprat, T., Fukuda, M., Grobe, H., Haeffelin, M., Hodges, G., Hyett, N., Ijima, O., Kallis, A., Knap, W., Kustov, V., Long, C. N., Longenecker, D., Lupi, A., Maturilli, M, Mimouni, M., Ntsangwane, L., Ogihara, H., Olano, X., Olefs, M., Omori, M., Passamani, L., Pereira E. B., Schmithüsen, H., Schumacher, S., Sieger, R., Tamlyn, J., Vogt, R., Vuilleumier, L., Xia, X., Ohmura, A., and König-Langlo, G.: Baseline Surface Radiation Network (BSRN): structure and data description (1992–2017). Earth Syst. Sci. Data, 10(3), 1491-1501. doi:10.5194/essd-10-1491-2018, 2018.

Ghimire, B., Williams, C. A., Masek, J., Gao, F., Wang, Z., Schaaf, C., and He, T.: Global albedo change and radiative cooling from anthropogenic land cover change, 1700 to 2005 based on MODIS, land use harmonization, radiative kernels, and reanalysis. Geophysical Research Letters, 41(24), 9087-9096. doi:https://doi.org/10.1002/2014GL061671, 2014.

Jia, A., Ma, H., Liang, S., and Wang, D.: Cloudy-sky land surface temperature from VIIRS and MODIS satellite data using a surface energy balance-based method. Remote Sensing of Environment, 263, 112566. doi:https://doi.org/10.1016/j.rse.2021.112566, 2021.

Jin, Y., Schaaf, C. B., Gao, F., Li, X., Strahler, A. H., Lucht, W., and Liang, S.: Consistency of MODIS surface bidirectional reflectance distribution function and albedo retrievals: 1. Algorithm performance. Journal of Geophysical Research: Atmospheres, 108(D5). doi:https://doi.org/10.1029/2002JD002803, 2003.

Lei F., Crow, W. T., Shen, H., Su, C., Holmes, T. R. H., Parinissa, R. M., and Wang, G.: Assessment of the impact of spatial heterogeneity on microwave satellite soil moisture periodic error, Remote Sens. Environ., vol. 205, pp. 85–99, 2018.

Li, X., Liu, Q., Yang, R., Wen, J., Zhang, J., Cai, E., and Zhang, H.: The Combination of Ground-Sensing Network and Satellite Remote Sensing in Huailai County. IEEE Sensors Journal, 16(10), 3819-3826. doi:10.1109/JSEN.2016.2535350, 2016.

Liang, S.: Narrowband to broadband conversions of land surface albedo I: Algorithms. Remote Sensing of Environment, 76(2), 213-238. doi:https://doi.org/10.1016/S0034-4257(00)00205-4, 2001.

Lin, X., Wu, S., Chen, B., Lin, Z., Yan, Z., Chen, X., Yin, G., You, D., Wen, J., Liu, Q., Xiao, Q., Liu, Q., and Lafortezza, R.: Estimating 10-m land surface albedo from Sentinel-2 satellite observations using a direct estimation approach with Google Earth Engine. ISPRS Journal of Photogrammetry and Remote Sensing, 194, 1-20. doi:https://doi.org/10.1016/j.isprsjprs.2022.09.016, 2022.

Loew, A., Bennartz, R., Fell, F., Lattanzio, A., Doutriaux-Boucher, M., and Schulz, J.: A database of global reference sites to support validation of satellite surface albedo datasets (SAVS 1.0). Earth Syst. Sci. Data, 8(2), 425-438. doi:10.5194/essd-8-425-2016, 2016.

Ma, M., Li, X., Weizhen, W., Xiao, Q., Zhao, K., and Xin, X.: Design on validation network of remote sensing products in China. ISPRS - International Archives of the Photogrammetry, Remote Sensing

https://doi.org/10.5194/essd-2023-220
Preprint. Discussion started: 12 July 2023

and Spatial Information Sciences, XL-2/W1, 1-6. doi:10.5194/isprsarchives-XL-2-W1-1-2013, 2013.

Marion, B.: Measured and satellite-derived albedo data for estimating bifacial photovoltaic system performance. Solar Energy, 215, 321-327. doi:https://doi.org/10.1016/j.solener.2020.12.050

Mcclean, F., Dawson, R., and Kilsby, C. (2020). Implications of Using Global Digital Elevation Models for Flood Risk Analysis in Cities. Water Resources Research, 56(10), 2021.

Moustafa, S. E., Rennermalm A. K., Román, M. O., Wang, Z., Schaaf, C. B., Smith, L. C., Koeing, L. S., and Erb, A.: Evaluation of satellite remote sensing albedo retrievals over the ablation area of the southwestern Greenland ice sheet, Remote Sens. Environ., vol. 198, pp. 115–125, 2017.

Pan, F., Wu, X., Tang, R., Zeng, Q., Li, Z., Wang, J., You, D., Wen, J., and Xiao, Q.: A coarse pixel scale ground "truth" dataset based on the global in situ site measurements from 2000 to 2021., Zenodo [dataset], https://doi.org/10.5281/zenodo.8008455, 2023.

Pinty, B., Lattanzio, A., Martonchik, J. V., Verstraete, M. M., Gobron, N., Taberner, M., Widlowski, J. L., Dickinson, R. E., and Govaerts, Y.: Coupling Diffuse Sky Radiation and Surface Albedo. Journal of the Atmospheric Sciences, 62(7), 2580-2591. doi:https://doi.org/10.1175/JAS3479.1, 2005.

Román, M. O., Schaaf, C .B., Woodcock, C .E., Strahler, A. H., Yang, X., Braswell, R. H., Curtis, P. S., Davis, K. J., Dragoni, Danilo., Goulden, M. L., Gu, L., Hollinger, D. Y., Kolb, T. E., Meyers, T. P., Munger, J. W., Privette, J. L., Richardson, A. D., Wilson, T. B., and Wofsy, S. C.: The MODIS (collection V005) BRDF/albedo product: Assessment of spatial representativeness over forested landscapes, Remote Sens. Environ., vol. 113, no. 11, pp. 2476–2498, 2009.

Rösel, A., and Kaleschke, L.: Comparison of different retrieval techniques for melt ponds on Arctic sea ice from Landsat and MODIS satellite data. Annals of Glaciology, 52(57), 185-191. doi:10.3189/172756411795931606, 2011.

Schaaf, C. B., Gao, F., Strahler, A. H., Lucht, W., Li, X., Tsang, T., Strugnell, Nicholas C., Zhang, Xiaoyang, Jin, Yufang, Muller, Jan-Peter, Lewis, Philip, Barnsley, Michael, Hobson, Paul, Disney, Mathias, Roberts, Gareth, Dunderdale, Michael, Doll, Christopher, d'Entremont, Robert P., Hu, Baoxin, Liang, Shunlin, Privette, Jeffrey L., and Roy, D.: First operational BRDF, albedo nadir reflectance products from MODIS. Remote Sensing of Environment, 83(1), 135-148. doi:https://doi.org/10.1016/S0034-4257(02)00091-3, 2002.

Song, R., Muller, J.-P., Kharbouche, S., and Woodgate, W.: Intercomparison of Surface Albedo Retrievals from MISR, MODIS, CGLS Using Tower and Upscaled Tower Measurements. Remote Sensing, 11(6). doi:10.3390/rs11060644, 2019.

Stokes, G. M., and Schwartz, S. E.: The Atmospheric Radiation Measurement (ARM) Program: Programmatic Background and Design of the Cloud and Radiation Test Bed. Bulletin of the American Meteorological Society, 75(7), 1201-1222. doi:https://doi.org/10.1175/1520-

https://doi.org/10.5194/essd-2023-220
Preprint. Discussion started: 12 July 2023

0477(1994)075<1201:TARMPP>2.0.CO;2, 1994.

Teixeira Pinto, C., Jing, X., and Leigh, L.:Evaluation Analysis of Landsat Level-1 and Level-2 Data Products Using In Situ Measurements. Remote Sensing, 12(16), 2597, 2020.

Uuemaa, E., Ahi, S., Montibeller, B., Muru, M., and Kmoch, A.: Vertical Accuracy of Freely Available Global Digital Elevation Models (ASTER, AW3D30, MERIT, TanDEM-X, SRTM, and NASADEM). Remote Sensing, 12(21), 3482, 2020.

Wang, K., and Liang, S.: Evaluation of ASTER and MODIS land surface temperature and emissivity products using long-term surface longwave radiation observations at SURFRAD sites. Remote Sensing of Environment, 113(7), 1556-1565. doi:https://doi.org/10.1016/j.rse.2009.03.009, 2009.

Wang, Z., Schaaf, C. B., Strahler, A. H., Chopping, M. J., Román, M. O., Shuai, Y., Woodcock, C. E., Hollinger, D. Y., and Fitzjarrald, D. R.: Evaluation of MODIS albedo product (MCD43A) over grassland, agriculture and forest surface types during dormant and snow-covered periods, Remote Sens. Environ., vol. 140, pp. 60–77, 2014.

Williamson M., Adams J. R., Berg A. A., Derksen C., Toose P., and Walker A.: Plot-scale assessment of soil freeze/thaw detection and variability with impedance probes: Implications for remote sensing validation networks, Hydrol. Res., vol. 49, no. 1, pp. 1–16, 2018.

Wu, X., Wen, J., Xiao, Q., Liu, Q., Peng, J., Dou, B., Li, X., You, D., Tang, Y., and Liu, Q.: Coarse scale in situ albedo observations over heterogeneous snow-free land surfaces and validation strategy: A case of MODIS albedo products preliminary validation over northern China. Remote Sensing of Environment, 184, 25-39. doi:https://doi.org/10.1016/j.rse.2016.06.013, 2016.

Wu, X., Wen, J., Xiao, Q., and You, D.: Upscaling of Single-Site-Based Measurements for Validation of Long-Term Coarse-Pixel Albedo Products. IEEE Transactions on Geoscience and Remote Sensing, 58(5), 3411-3425. doi:10.1109/TGRS.2019.2954879, 2020.

Wu, X., Wen, J., Xiao, Q., You, D., Gong, B., Wang, J., Ma, D., and Lin, X.: Spatial Heterogeneity of Albedo at Subpixel Satellite Scales and its Effect in Validation: Airborne Remote Sensing Results From HiWATER. IEEE Transactions on Geoscience and Remote Sensing, 60, 1-14. doi:10.1109/TGRS.2021.3124026, 2022.

Wu, X., Xiao, Q., Wen, J., You, D., and Hueni, A.: Advances in quantitative remote sensing product validation: Overview and current status. Earth-Science Reviews, 2019.

Xu, B., Li, J., Park, T., Liu, Q., Zeng, Y., Yin, G., Zhao, J., Fan, W., Yang, L., Knyazikhin, Y., Myneni, R. B.: An integrated method for validating long-term leaf area index products using global networks of site-based measurements, Remote Sens. Environ., vol. 209, pp. 134–151, 2018.

Yamazaki, D., Ikeshima, D., Tawatari, R., Yamaguchi, T., O'Loughlin, F., Neal, J. C., Sampson, C. C., Kanae, S., and Bates, P. D.: A high-accuracy map of global terrain elevations. Geophysical Research Letters, 44(11), 5844-5853. doi:10.1002/2017gl072874, 2017.

https://doi.org/10.5194/essd-2023-220
Preprint. Discussion started: 12 July 2023

Open Access Earth System Science Data Discussions

Zhou, Y., Wang, D., Liang, S., Yu, Y., and He, T.: Assessment of the Suomi NPP VIIRS Land Surface Albedo Data Using Station Measurements and High-Resolution Albedo Maps. Remote Sensing, 8(2), 137, 2016.